SUPERBUBBLES AS SPACE BAROMETERS

G. GARCIA-SEGURA[1] AND M. S. OEY[2,3]

[1] Instituto de Astronomía, Universidad Nacional Autónoma de México, Apartado Postal 877, Ensenada, 22830
Baja California, Mexico
E-mail: ggs@astrosen.unam.mx

[2] Lowell Observatory, 1400 West Mars Hill Rd., Flagstaff, AZ   86001, USA

[3] Department of Astronomy, 830 Dennison Building, University of Michigan, Ann Arbor, MI   48109-1090, U.S.A.
E-mail: msoey@umich.edu

ABSTRACT

High ambient interstellar pressure is suggested as a possible factor to explain the ubiquitous observed growth-rate discrepancy for supernova-driven superbubbles and stellar wind bubbles. Pressures of $P/k \sim 10^5$ cm^{-3} K are plausible for regions with high star formation rates, and these values are intermediate between the estimated Galactic mid-plane pressure and those observed in starburst galaxies. High-pressure components also are commonly seen in Galactic ISM localizations. We demonstrate the sensitivity of shell growth to the ambient pressure, and suggest that superbubbles ultimately might serve as ISM barometers.

Key words : galaxies: ISM — Magellanic Clouds — ISM: bubbles — ISM: general — supernova remnants

I. INTRODUCTION

Why Superbubbles are smaller and slower than predicted ?

One problem that is empirically well-established is the result that most superbubbles apparently grow more slowly than expected. This has been observed in individual stellar wind bubbles such as Wolf-Rayet nebulae (Treffers & Chu 1982; García-Segura & Mac Low 1995; Drissen et al. 1995), as well as in superbubbles powered by OB associations (e.g., Oey 1996a; Oey & Smedley 1998; Brown et al. 1995; Saken et al. 1992). This growth-rate discrepancy has been identified in young, nebular shell systems, in which the parent OB association is still present; thus the input mechanical power is well-constrained. The discrepancy is seen both in objects that show no evidence of previous supernova activity, and in ones where one or two supernovae have already exploded (Oey 1996a; hereafter O96).

The classical solution for the evolution of wind blown bubbles is obtained by asuming nule ISM pressure ($P_e = 0$) and solving the system:

$$\frac{d}{dt}\left(M_s \dot{R}\right) = 4\pi R^2 P_i \qquad (1)$$

$$\frac{dE}{dt} = L_w - \frac{dV}{dt} P_i \qquad (2)$$

where P_i is the interior bubble pressure, M_s, E, and V are the shell mass, interior energy, and interior volume. R is the shell radius and L_w is the wind mechanical

luminosity. For constant input mechanical power L_w and ambient number density n, the evolution of the shell radius is given by (e.g., Castor, McCray, & Weaver 1975; Weaver et al. 1977):

$$R = 68.9 \ (L_{38}/n)^{1/5} \ t_6^{3/5} \ \text{pc} \quad, \qquad (3)$$

where L_{38} is L_w in units of 10^{38} erg s^{-1}, and t_6 is age of the bubble in Myr. The shell expansion velocity $v = \dot{R}$ is the time derivative of equation 3.

One possible solution to the growth-rate discrepancy suggests that the input parameter L/n is systematically overestimated. For eight nebular superbubbles with well-constrained R, v, L_w, and t, Oey and collaborators (O96; Oey & Massey 1995; Oey & Smedley 1998) showed that L/n would need to be reduced by a factor of several, perhaps up to an order of magnitude, to reconcile the observations with prediction. Since stellar wind power L is sensitive to the stellar mass, a substantial uncertainty in L is not unreasonable. As shown by multi-wavelength observations of three of the superbubbles (Oey et al. 2002), the multi-phase ambient ISM also renders n similarly uncertain. However, the implication of a systematic growth-rate discrepancy remains difficult to explain.

The superbubbles studied by Oey and collaborators are all located in the Large Magellanic Cloud (LMC). For these objects, Silich & Franco (1999) suggested that the ambient environment and viewing geometry conspire to yield misleading observed shell dynamics. They suggest that the superbubbles are more extended perpendicular to the galaxy's plane, as would be expected in the plane-stratified density distribution of disk galaxies (but see also Maciejewski & Cox 1999).

The elongation of the shells would not be apparent because of the LMC's almost face-on orientation. While this is an attractive suggestion for the LMC objects, it does not explain the growth-rate discrepancy seen in Galactic (e.g., Brown et al. 1995; Saken et al. 1992) and M33 (Hunter et al. 1995) objects.

Nevertheless, it is apparent that the ambient environment plays a crucial role in the superbubble growth and evolution. In addition to the work of Silich & Franco (1999), other studies have shown that the shell dynamics are sensitive to the ambient density structure (e.g., Oey & Smedley 1998; Mac Low et al. 1998). Multi-wavelength observations also show that the ambient multiphase gas distribution is difficult to constrain without direct such observations (Oey et al. 2002).

Continuing to focus on the ambient environment, this present work now investigates the effect of the ambient pressure. Since most superbubble growth is eventually expected to become confined by the ambient interstellar pressure (Oey & Clarke 1997), this parameter is also worth examining more closely. We note that Dopita et al. (1981) suggested an active pressure mechanism to confine the shell of one LMC object by invoking exterior ram pressure caused by contraction of a surrounding interstellar cloud. Here, we suggest that the typical interstellar pressures in some systems may be higher than assumed.

When the ISM pressure is included in the study ($P_e \neq 0$), one gets the next system to solve:

$$\frac{d}{dt}\left(M\dot{R}\right) = 4\pi R^2 \left(P_i - P_e\right) \qquad (4)$$

$$\frac{dE}{dt} = L_{\mathrm{w}} - \frac{dV}{dt}\left(P_i - P_e\right) \qquad (5)$$

where P_i and P_e are the interior and exterior pressure, respectively. Unfortunately, there are not anlytical solutions like equation (3), since the system is not self-similar.

In earlier work, Oey used a simple, semi-analytic, 1-D model that integrates the shell's equations of motion. The model is described in detail by Oey & Massey (1995) and O96. For their sample of eight young, nebular superbubbles, they tailored the model input parameters (L, n, t) according to the individual, empirically-derived values. As mentioned above, these highly constrained models confirm the ubiquitous growth-rate discrepancy between the observed and predicted shell radius and expansion velocity (e.g., O96). In above studies, the ambient interstellar pressure P_e was estimated as $P_e = \rho c_s^2/\gamma$. The soundspeed c_s was usually estimated as 10 km s^{-1} for ionized nebular gas, provided that R remains smaller than the Strömgren radius; ρ is the mass density; and γ is the equation of state index, which was taken to be 5/3 for the adiabatic condition. For n ranging between 1 and 10 cm^{-3}, as estimated for our objects, this yields $P_e/k = 9 \times 10^3$ to 9×10^4 cm^{-3} K.

For the Milky Way, the total mid-plane ISM pressure is generally estimated to be around $P/k \sim 3 \times 10^4$ cm^{-3} K. This includes roughly equal empirical contributions from the diffuse thermal pressure, magnetic field pressure, non-thermal velocity field or turbulent pressure, and cosmic ray pressure; a good discussion is presented by Slavin & Cox (1993). This value is consistent with the constraint derived by Boulares & Cox (1990) that the pressure required to support the weight of the Galactic ISM is $P/k \sim 2.8 \times 10^4$ cm^{-3} K.

In recent years, turbulent velocity structure is becoming more quantified as one of the major, and perhaps dominant, kinematic properties of the ISM in star-forming galaxies. This is linked to a new paradigm shift for the ISM to less distinct thermal phases, in which cool clouds are transient, unconfined features, rather than distinct and well-defined entities (Vázquez-Semadeni 2002; Kritsuk & Norman 2002). This turbulence-dominated view of the ISM implies a strong presence of components and localizations that are not in pressure equilibrium (Mac Low et al. 2001; Kim et al. 2001). Such components are now being ubiquitously identified in thermal pressure distributions determined for lines of sight to Galactic stars (Jenkins & Tripp 2001; Wallerstein et al. 1995), where these are found to have thermal $P_{\mathrm{th}}/k \gtrsim 10^5$ cm^{-3} K. Also note that the turbulent pressure $P_{\mathrm{tb}}/k \simeq \rho\sigma_v^2/k \sim 7.5 \times 10^4$ cm^{-3} K for the hot, ionized medium (HIM) if we consider values of $n \sim 0.05$ cm^{-3} and turbulent velocity dispersion $\sigma_{\mathrm{v}} \sim c_s \sim 100$ km s^{-1}. The magnetic field pressure also shows occasional hints for high-value components (e.g., Edgar & Cox 1993). On the other hand, the cosmic ray pressure contribution may be less relevant to confining superbubble growth since the shells may be transparent to cosmic rays (Slavin & Cox 1993).

The above factors apply to the Milky Way, which is a giant disk galaxy whose midplane ISM pressure should be substantially higher than in a Magellanic irregular galaxy like the LMC, where all of our sample objects are located. Thus, one could argue that P_e estimated by our earlier models are already on the high side of what might be expected. On the other hand, several of the pressure terms, namely, the thermal, turbulent, and cosmic ray pressures, should scale with star formation rate (SFR) per unit volume. Thermal pressures within star forming regions themselves are of order $P_{\mathrm{th}}/k \sim 10^5 - 10^6$ cm^{-3} K (e.g., Malhotra et al. 2001), and superbubbles generally originate within such regions, although presumably they outgrow and outlive them. For a high filling factor or interstellar porosity generated by the superbubble activity, it is also quite likely that the magnetic pressure is also determined by the SFR. The magnetic field strength is correlated with gas density, yielding localized values of order a few hundred μG in Galactic molecular clouds and star-forming regions (Crutcher 1999). The expansion of superbubbles themselves also compresses the magnetic field, causing a self-induced im-

TABLE 1
LMC SUPERBUBBLE PARAMETERS[a]

DEM	R (pc) [b]	v ($\mathrm{km\,s^{-1}}$) [c]	$\log Q^0$ ($\log \mathrm{s^{-1}}$) [d]	120 $M_\odot$ $\tau = 3.12$	85 $M_\odot$ $\tau = 3.48$	60 $M_\odot$ $\tau = 4.12$	40 $M_\odot$ $\tau = 5.26$	25 $M_\odot$ $\tau = 7.84$	20 $M_\odot$ $\tau = 9.96$
				Pre-SN superbubbles					
L31	50	30:	50.161	1	0	0	1	4	2
L106	30	$\lesssim 10$	49.745	0	1	0	2	0	4
L226	28	$\lesssim 5$	49.403	0	0	1	1	0	1
				Post-SN superbubbles[e]					
L25	43	60:	48.459	0	0	0 (1)	0 (1)	2	2
L50	50	25	49.342	0	0 (1)	0 (1)	3	1	7
L301	53	40:	50.310	0	0	0 (1)	3	3	1

[a]Data compiled by O96). Columns 6–11 represent numbers of stars in each mass bin; expected lifetime in Myr is shown in the column heading.

[b]Uncertainty $\sim 10 - 15\%$.

[c]Objects with ":" uncertain to 50%, but see text; others $\sim 20\%$. See O96 for source references for v.

[d]Uncertainty of order a factor of 2.

[e]Values in parentheses show original number of stars implied by the IMF, from O96.

pedance (Slavin & Cox 1992). On large scales, radio synchrotron measurements for other galaxies are showing magnetic field strengths of ~ 15 μG in actively star-forming galaxies, and up to 40 μG in spiral arms (Beck 2004). Such values imply magnetic pressures alone of order $P_B/k \sim 10^5$ cm^{-3} K.

The LMC has one of the highest SFR per unit volume in the Local Group. Its interstellar porosity Q is exceeded only by that of IC 10 (Oey et al. 2001), although Q for the Milky Way is difficult to determine. Taking the SFR consistently estimated from the H II region luminosity function for both the Galaxy (Oey & Clarke 1997) and the LMC (Oey et al. 2001), we obtain porosities of $Q \sim 0.3$ and 1, respectively. The formal Q for IC 10 is an order of magnitude higher yet. Thus it is not unreasonable that the LMC may have total interstellar pressures that are similar to, or in excess of, those of the Milky Way. We can also compare with the central few kpc of nuclear starburst galaxies like M82, which have empirically determined $P/k \sim 10^6$ cm^{-3} K (e.g., Lord et al. 1996). If the Milky Way ISM, with $P/k \sim 10^4$ cm^{-3} K, is typical for ordinary star-forming galaxies, then galaxies with SFR intermediate between "ordinary" and starburst, like the LMC, should be expected to likewise have interstellar pressures that are intermediate, namely, of order $P/k \sim 10^5$ cm^{-3} K. Equations (4) and (5) shows that such values would be significant in counteracting the pressure-driven shell growth.

II. MODELS OF LMC SUPERBUBBLE EVOLUTION

In light of the above, it is worth further exploring the effects of the ambient pressure parameter on the superbubble evolution. A study of the evolution of wind blown bubbles and HII regions in large ambient pressures can be found in García-Segura & Franco (1996). We return to the same LMC objects studied by O96 (Fig. 1), now modeling these with 1-D hydrodynamical computations using the magneto-hydrodynamic fluid solver ZEUS-3D (version 3.4). This code is the updated, 3-D version of the two-dimensional code ZEUS-2D (Stone & Norman 1992), an Eulerian explicit code which integrates the equations of hydrodynamics for a magnetized ideal gas. The code also works efficiently in one dimension, and we perform the simulations in spherical coordinates, with 1000 zones in the radial direction r. Taking the time-dependent stellar wind mechanical luminosity $L(t) = \frac{1}{2} \dot{M}(t)\, v_\infty^2$ for each object from O96, we assume a constant terminal velocity $v_\infty = 3000$ km s^{-1}, yielding a wind density $\rho(t) = \dot{M}(t)/4\pi r^2 v_\infty$, where $\dot{M}(t)$ is the wind mass-loss rate. O96 estimated $L(t)$ from the observed and inferred stellar population (Table 1, below) based on empirical relations between wind properties and spectral type, and evolutionary models. The time-dependent wind conditions are set within the first few radial computational zones, centered at the origin.

ZEUS-3D does not include radiation transfer, but we have implemented a simple approximation to derive

the location of the ionization front for arbitrary density distributions (see Bodenheimer et al. 1979). This is done by assuming that ionization equilibrium holds at all times, and that the gas is fully ionized inside the HII region. The position of the ionization front is given by $\int n^2(r)r^2 dr \approx Q^0/4\pi\alpha_B$, where Q^0 is the stellar H-ionizing emission rate and α_B is the Case B recombination coefficient.

The models include the Raymond & Smith (1977) cooling curve above 10^4 K. For temperatures below 10^4 K, the shocked gas region is allowed to cool down with the radiative cooling curves given by Dalgarno & Mc-Cray (1972) and MacDonald & Bailey (1981). Finally, the photoionized gas is always kept at 10^4 K , so no cooling curve is applied to the HII regions (unless there is a shock inside the photoionized region).

We assume an initially homogeneous ISM, which supplies the external pressure. Given the existence of large non-thermal "turbulent" velocities, of several km s^{-1}, cosmic rays and magnetic fields, the *total* pressure should be obviously a combination of all of them, as discussed above. However, to simplify computation, we model the total ambient pressure as originating entirely from thermal pressure. Thus, in order to have thermal pressures of $P/k = 1 \times 10^5$ cm^{-3} K, we adopt for the ISM density $n \sim 16.7$ cm^{-3} and 6000 K for the temperature. This gives us a sound speed of $c_{s,\mathrm{isoth}} \sim 7$ km s^{-1}. For a second set of models with $P/k = 1 \times 10^4$ cm^{-3} K, we use an ISM density of $n \sim 1.67$ cm^{-3} and 6000 K for the temperature.

Table 1 gives the observed nebular radius R, nebular expansion velocity v, and Q^0 in columns 2 – 4, respectively, for the sample objects. Columns 5 – 10 give the observed and pre-SN inferred massive star population down to $20\,M_\odot$. O96 describes how the input mechanical power $L(t)$ due to stellar winds and SNe is estimated from the individual massive star populations as a function of time. Figures 1 and 2 of O96 show that $L(t)$ for these objects typically have early values of $10^{37} - 10^{39}$ erg s^{-1}. All parameters are listed in Table 1 as measured and compiled from the literature by O96, except for Q^0, which is estimated by Oey & Kennicutt (1997). The objects are divide into "Pre-SN" and "Post-SN" categories: the Pre-SN objects show no enhanced X-ray emission or enhanced [S II]/Hα ratios, thus are presumed to have no prior SN activity. Objects listed as Post-SN show both enhanced X-ray emission (Chu & Mac Low 1990; Wang & Helfand 1991) and [S II]/Hα, indicating recent SN impacts on the shell walls; the masses of the SN progenitors are estimated from the stellar initial mass functions (IMF) and included in $L(t)$ for the models, as done by O96.

Figure 1 shows the emission measure of our new models for the photoionized gas, using the input $L(t)$ determined by O96 from the observed stellar population (Table 1) of the individual LMC objects. These models adopt a high ambient pressure $P/k = 1 \times 10^5$ cm^{-3} K. As discussed earlier, contributions from

turbulent, magnetic, and multi-phase thermal pressure terms would presumably contribute to such high ambient values. The snapshots are those corresponding to the observed radii in Table 1, with Pre-SN objects shown in the left column, and Post-SN objects shown on the right. The evolution times of the snapshots are: 2.6 Myr (L31), 2 Myr (L106), 2.8 Myr (L226), 4.4 Myr (L25), 5.6 Myr (L50) and 4.6 Myr (L301).

Comparison with Table 1 shows that the high-pressure models are in good agreement with the observed parameters in all cases: the predicted ionized radius, expansion velocity, and age are all reasonably consistent with the observed values. In Figure 1 we also reproduce Hα images of the superbubbles from Figure 1 of Oey (1996b). Figure 1 shows that the putative Pre-SN objects DEM L106 and L226 show thicker nebular shells, of order 10% of R, whereas the post-SN objects show compressed, filamentary morphology. DEM L31, presumed to be Pre-SN, is also quite filamentary, and the model also reproduces this structure, owing primarily to its high input power (Table 1). This is fully consistent with the predicted morphology of the ionized regions in the models.

The velocity profiles (not shown here) (see Oey & García-Segura 2004) also imply observed velocities that are reasonably consistent with the data (Table 1). The latter are especially complex for the most filamentary objects, showing velocity components that vary by factors of 2–3. This is consistent with the extreme gradients in both density and velocity seen in the models. DEM L31 and DEM L301 show a significant range in velocity, and maximum values consistent with those observed. Predicted velocities for the remaining objects are also consistent with the observed upper limits. We note that both observations and models are likely to be sensitive to details of geometry and ionization in the post-SN objects, since complex shock structures are generated on short timescales. Thus it is unsurprising that the model velocity profiles tend to be more simplistic than the observations. We also see that the models for DEM L25 and DEM L50 imply that the ionization front does not penetrate the high-density shell; however, observations of these objects do show high-density, filamentary structure that is fully ionized for DEM L25, and mostly ionized for DEM L50 (Oey et al. 2002). Oey & Kennicutt (1997) find excess in the nebular emission, by factor of a few, beyond what can be attributed to stellar photoionization. Thus, shock excitation is likely to enhance the ionized mass and radius of these objects. Nevertheless, the broad agreement in the dominant shell parameters across the sample demonstrates that *a high ambient pressure alone can solve the growth-rate discrepancy* that is widely observed in such objects.

We also compare with similar models assuming a lower ambient pressure of $P/k = 1 \times 10^4$ cm^{-3} K, implemented as described above. While this ambient P/k value is more consistent with standard expectations, it is apparent that the models (see Oey & García-Segura
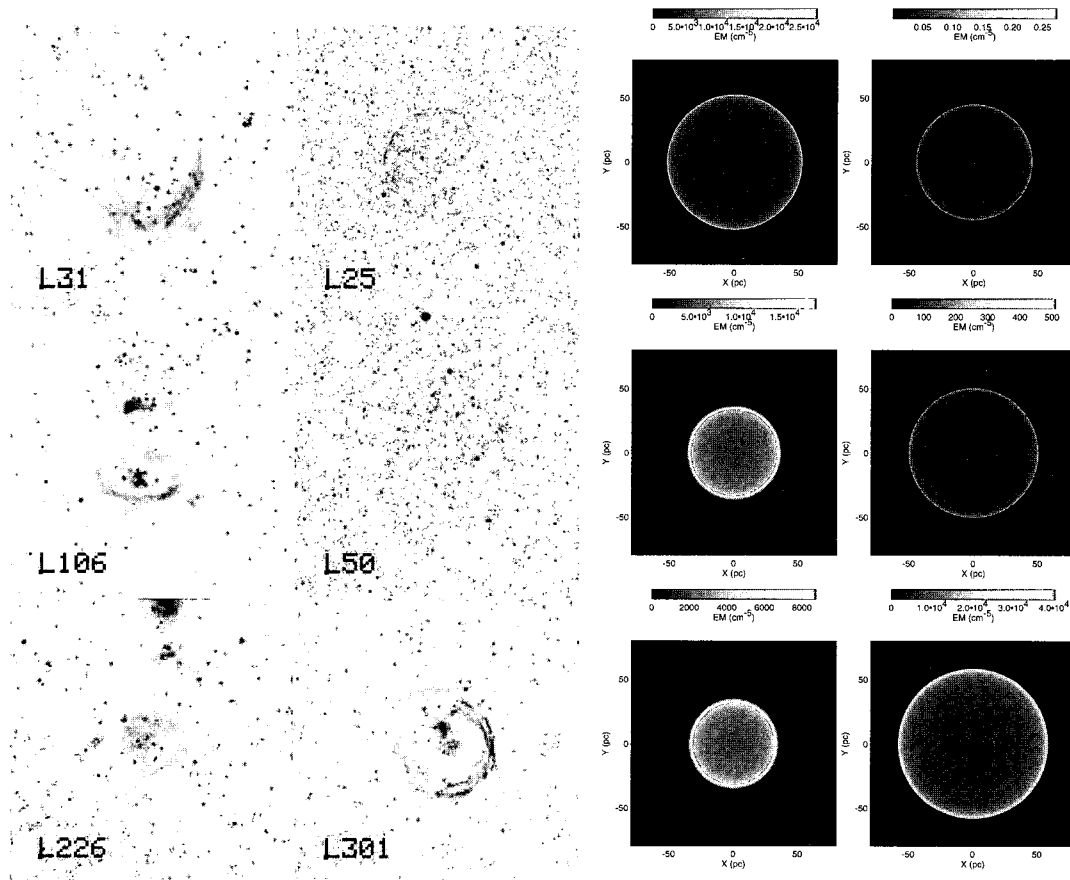
Fig. 1.— (Left) Hα images of the LMC superbubbles, from Oey (1996b). Each image is 16.$'$67 square. (Right) Emission measure of models assuming an ambient $P/k = 1 \times 10^5$ cm^{-3} K, for R corresponding to the observed values. The evolution times of the snapshots are: 2.6 Myr (L31), 2 Myr (L106), 2.8 Myr (L226), 4.4 Myr (L25), 5.6 Myr (L50) and 4.6 Myr (L301).

2004) are in poor agreement with the data. The collective ages are systematically too young, thus demonstrating the ubiquitous growth-rate discrepancy, and the predicted shell parameters are more difficult to reconcile with the observations. Since none of the objects have reached the SN stage, the Post-SN objects retain thick, extended shells. Indeed, all but one of the objects are predicted to have a surrounding ionized halo that is at most a factor of 3 lower in density than the inner shell; these halos are not observed. Another especially interesting feature in these models is the appearance of a double shell structure: a second, neutral shell is seen at roughly 2 – 3 times the radius of the ionized inner shell. This outer shell results from the expansion of the photoionized H II region in a D-type ionization front. Oey et al. (2002) presented H I observations of the three post-SN objects (DEM L25, DEM L50, and DEM L301), at a spatial resolution of 50$''$ (12.5 pc); they found no apparent evidence of such secondary shells. The existence of neutral secondary shells could potentially offer a diagnostic of lower ambient pressures.

III. CONCLUSIONS

Our models clearly show that increasing the ambient interstellar pressure by an order of magnitude, from $P_e/k = 1 \times 10^4$ to 1×10^5 cm^{-3} K, can impede the shell growth to a degree that could fully account for the observed growth-rate discrepancy. In §1, we presented arguments that such high interstellar pressures could exist, especially based on the dependence of P_e on star-formation rate. While other factors mentioned in §1, namely, overestimated L/n and viewing geometry, could all be additional factors that contribute to the growth-rate discrepancy, we note that the multi-phase gas morphology is more consistent with high interstellar pressure dominating this effect.

Finally, as noted by Oey & Clarke (1997), the assumed global value of P_e plays a critical role in determining the characteristic final sizes of old, SN-dominated superbubbles, and hence, the superbubble size distribution, which is dominated by pressure-confined shells. This, in turn, determines the interstellar porosity and filling factor of the hot, ionized

medium in star-forming galaxies. With adequate clarification in the superbubble evolution process and input parameters, the superbubble sizes, kinematics, and morphologies could potentially provide barometers for the interstellar pressure. These diagnostics could be especially useful in other galaxies, which have fewer available empirical pressure indicators than the Milky Way.

REFERENCES

Beck, R. 2004, in *From Observations to Self-Consistent Modelling of the ISM in Galaxies*, eds. M. A. de Avillez & D. Breitschwerdt, Ap&SS, 289, 293

Bodenheimer, P., Tenorio-Tagle, G., & Yorke, H. W. 1979, ApJ, 233, 85

Boulares, A., & Cox, D. P. 1990, ApJ, 365, 544

Brown, A. G. A., Hartmann, D., & Burton, W. B. 1995, A&A, 300, 903

Castor, J. I., McCray, R., & Weaver, R., 1975, ApJ, 200, L107

Chu, Y.-H. & Mac Low, M-M., 1990, ApJ, 365, 510

Crutcher, R. M., 1999, ApJ, 520, 706

Dalgarno, A. & McCray, R. A. 1972, ARAA, 10, 375

Dopita, M. A., Ford, V. L., McGregor, P. J., Mathewson, D. S., & Wilson, I. R., 1981, ApJ, 250, 103

Drissen, L., Moffat, A. F. J., Walborn, N. R., & Shara, M. R. 1995, AJ, 110, 2235

Edgar, R. J. & Cox, D. P. 1993, ApJ, 413, 190

García-Segura, G. & Franco, J. 1996, ApJ, 469, 171

García-Segura, G. & Mac Low, M.-M. 1995, ApJ, 455, 145

Hunter, D. A., Boyd, D. M., & Hawley, W. N. 1995, ApJS, 99, 551

Jenkins, E. B. & Tripp, T. M. 2001, ApJS, 137, 297

Kim, J., Mac Low, M.-M., & Balsara, D. S. 2001, JKAS, 34, 333

Kritsuk, A. G. & Norman, M. L. 2002, ApJ, 569, L127

Lord, S. D., Hollenbach, D. J., Haas, M. R., Rubin, R. H., Colgan, S. W. J., & Erickson, E. F. 1996, ApJ, 465, 703

Maciejewski, W. & Cox, D. P. 1999, ApJ, 511, 792

MacDonald, J., & Bailey, M. E. 1981, MNRAS, 197, 995

Mac Low, M.-M., Balsara, D. S., de Avillez, M. A., & Kim, J. 2001, BAAS, 198, #65.10

Mac Low, M.-M., Chang, T. H., Chu, Y.-H., Points, S. D., Smith, R. C., & Wakker, B. P. 1998, ApJ, 493, 260

Malhotra, S., et al. 2001, ApJ, 561, 766

Oey, M. S. 2004, in *From Observations to Self-Consistent Modelling of the ISM in Galaxies*, eds. M. A. de Avillez & D. Breitschwerdt, Ap&SS, 289, 269

Oey, M. S. 1996a, ApJ, 467, 666 (O96)

Oey, M. S. 1996b, ApJ, 465, 231

Oey, M. S., & Clarke, C. J. 1997, MNRAS, 289, 570

Oey, M. S., & García-Segura, G. 2004, ApJ, in press

Oey, M. S., Groves, B., Staveley-Smith, L., & Smith, R. C. 2002, AJ, 123, 255

Oey, M. S., Clarke, C. J., & Massey, P. 2001, in *Dwarf Galaxies and Their Environment*, eds. K. S. de Boer, R.-J. Dettmar, & U. Klein, Shaker Verlag, 181.

Oey, M. S. & Kennicutt, R. C. 1997, MNRAS, 291, 827

Oey, M. S. & Massey, P., 1995, ApJ, 452, 210

Oey, M. S. & Smedley, S. A. 1998, AJ, 116, 1263

Raymond, J. C., & Smith, B. W. 1977, ApJS, 35, 419

Saken, J. M., Shull, J. M., Garmany, C. D., Nichols-Bohlin, J., & Fesen, R. A. 1992, ApJ, 397, 537

Silich, S. A. & Franco, J. 1999, ApJ, 522, 863

Slavin, J. D. & Cox, D. P. 1992, ApJ, 392, 131

Slavin, J. D. & Cox, D. P. 1993, ApJ, 417, 187

Stone, J. M. & Norman, M. L. 1992, ApJS, 80, 753

Treffers, R. R. & Chu, Y.-H. 1982, ApJ, 254, 569

Vázquez-Semadeni, E. 2002, in *Seeing Through the Dust: The Detection of H I and the Exploration of the ISM in Galaxies*, eds. R. Taylor, T. Landecker, & A. Willis, (San Francisco: ASP), 155

Wallerstein, G., Vanture, A., & Jenkins, E. B. 1995, ApJ, 455, 590

Wang, Q. & Helfand, D. J. 1991, ApJ, 373, 497

Weaver R., McCray R., Castor J., Shapiro P., Moore R. 1977, ApJ, 218, 377